Materials Science and Engineering A 529 (2011) 131–137

Contents lists available at SciVerse ScienceDirect

Materials Science and Engineering A

journal homepage: www.elsevier.com/locate/msea

Extruded Al–Al_2O_3 composites formed in situ during consolidation of ultrafine Al powders: Effect of the powder surface area

Martin Balog[a,*], Frantisek Simancik[a], Martin Walcher[b], Walter Rajner[b], Cecilia Poletti[c]

[a] The Institute of Materials and Machine Mechanics, Slovak Academy of Sciences, Bratislava, Slovakia
[b] NMD – New Materials Development GmbH, St. Pantaleon, Austria
[c] Institute of Materials Science and Welding, Graz University of Technology, Kopernikusgasse 24/I, A8010 Graz, Austria

ARTICLE INFO

Article history:
Received 7 July 2011
Received in revised form 31 August 2011
Accepted 2 September 2011
Available online 8 September 2011

Keywords:
Aluminium
Extrusion
Metal matrix composites
Powder metallurgy
SAP

ABSTRACT

Twenty-five samples of commercially available, gas-atomised Al (99.5%) powders with particle sizes <10 μm were hot extruded into Al–Al_2O_3 composites formed in situ during extrusion. The effect of particle size, surface area, oxygen content and atomisation atmosphere of the powder on the microstructure and mechanical properties of the extruded compacts were studied by Brunauer, Emmett, Teller (BET) analysis, hot gas extraction, scanning electron microscopy (SEM), electron backscatter diffraction (EBSD), transmission electron microscopy (TEM) and tensile tests. Thermal stability of the compacts and the individual strengthening mechanisms operating in the compacts were discussed. It was found that the properties of the compacts stemmed from the extraordinary grain boundary strengthening effect of the ultrafine-grained compacts due to their microstructures. The efficiency of the grain boundary strengthening was significantly enhanced by the presence of nano-metric Al_2O_3 dispersoids introduced in situ. The strength of the compacts was closely related to the surface area of the powder particles. In addition, the entrapped gasses and chemically bonded humidity had a negative effect on the mechanical properties of the compacts.

1. Introduction

Sintered aluminium pulver (SAP) materials offer superior mechanical properties, enhanced creep performance and increased thermal stability at elevated temperatures after prolonged high temperature exposures [1–3]. SAP materials include a broad range of dispersion-strengthened Al–Al_2O_3 composites produced primarily from mechanically milled or further oxidised Al powders [4–7]. However, the mechanical properties of these compacts cannot be reliably reproduced, and they have high production costs, problems with removing the process control agent (PCA) used during milling and inferior plasticity. These issues prohibited the widespread use of SAP in the last century. Nowadays, atomised Al powders are readily available at industrially relevant quantities and price levels. By compacting finely atomised Al powders, the Al_2O_3 phase can be introduced into the material in situ to produce ultrafine-grained Al–Al_2O_3 composites [8]. This Al_2O_3 phase originated from the thin oxide film present on the surface of the as-atomised powder. Despite the small volume of the Al_2O_3 phase (typically <3 vol%), the compacts have excellent thermal stability and mechanical properties. A need for new and lightweight materials with enhanced thermal stability, in areas such as the automotive industry, opens new potential for employing the finely atomised Al powders to produce SAP-like materials.

To utilise the finely atomised Al powders, they need to be consolidated by induced plastic deformation. Commonly used consolidation methods, such as sintering and hot isostatic pressing (HIP), should be avoided because they cause grain growth and spheroidisation of dispersed oxides, which are detrimental to the mechanical properties of the powders [8]. To obtain sufficient ductility and toughness in the compacts, the atomised Al powders need to be plastically deformed using shear forces. Shearing enlarges the surface of the powders, which breaks up the Al_2O_3 film present on the surface of the as-atomised Al powders significantly. Hot direct extrusion (DE) is the most frequently used technique because: (i) the technique has high productivity; (ii) the technique is based on Al ingot extrusion, an established technique; (iii) the shape of the final 2D profile has high dimensional preciseness; (iv) the extruded profiles have large cross sections; (v) the technique produces very small residual porosity; (vi) a broad range of Al alloys can be extruded; (vii) the technique requires relatively low processing temperature, which reduces undesired reactions, coarsening and translates into energy savings and (viii) the technique induces intensive shear deformation that refines and homogenises the final structure. In many aspects, extrusion consolidation surpasses consolidation by sintering, which is very problematic in the case of

* Corresponding author. Tel.: +421 2 59309414; fax: +421 2 44253301.
E-mail addresses: martin.balog@savba.sk, ummsbama@savba.sk (M. Balog).

0921-5093/$ – see front matter © 2011 Elsevier B.V. All rights reserved.
doi:10.1016/j.msea.2011.09.006

Al-based powders. Conversely, sintering is cost effective and can fabricate the (near) net shape of complex 3D parts. Nevertheless, the market share for extruded Al-based powder products is still small compared to that for sintered products. Avoiding complicated, time-consuming and expensive pre-processing steps of canning and/or hot isostatic pressing, widely used prior to extrusion, would make extrusion consolidation more competitive. As shown in [4,8,9] and in industrial applications [10,11], these pre-processing steps can be successfully avoided without affecting the high temperature mechanical properties of the compacts.

In this study, 25 samples of commercially available, gas-atomised Al (99.5%) powders from eleven different manufacturers with particle sizes below 10 μm were hot extruded into SAP-like compacts in the laboratory. The commercial powders that were used represented the finest Al powder size fractions offered on the market, available in quantities acceptable for industrial use. To keep the approach presented in this work economically competitive, the pre-processing steps including powder canning and/or hot isostatic pressing were avoided prior to extrusion. The main aim was to evaluate the effect of the Al powder properties (particle size, particle surface area, oxygen content, atomisation atmosphere) on the mechanical properties of the extruded compacts. This study was a continuation of the research on the synthesis and characterisation of fine Al powder compacts [4,8,9,12].

2. Experimental

The powders used for this study were gas-atomised from a technical purity (Al > 99.5 wt%) melt. The powders were atomised or collected under either nitrogen (18 samples) or air (7 samples). All powders were supplied by *NMD G.m.b.H.* [11]. The powder surface area was determined by physical adsorption with multi-point Brunauer, Emmett, Teller (BET) analysis using nitrogen gas according to ISO 9277. The mean particle size of the powders (d_{50}) was analysed by a Sympatec HELOS laser diffraction system by dry dispersion. The oxygen content of 21 as-atomised powders was measured immediately after atomisation by hot gas extraction using Ströhlein machine. The equivalent BET diameter (d_{BET}) was calculated according to the relation $d_{BET} = 6/(BET \times \rho_{Al})$, where ρ_{Al} is the density of Al. The Al_2O_3 dispersoids volume was calculated from oxygen content detected on as-atomised powders. All detected oxygen was assumed to be present within Al_2O_3. The fact that some oxygen was present in the form of bonded humidity and some additional oxidation takes place during green compacts heating and extrusion process was neglected. The properties of as-atomised Al powders are summarised in Table 1. The different Al powder manufacturers were labelled with different numbers.

40 grams of loose powder was cold isostatically pressed (CIP) at 200 MPa. The pressed powders were filled in an extrusion container with a diameter of 20 mm and preheated to the extrusion temperature, and the container was held at temperature for 30 min. The powders in the die were then directly extruded into a rod with a circular cross section using a laboratory extruder with a 180° nozzle die. Extrusion was carried out at 450 °C with an extrusion ratio of $R = 11{:}1$ and an average ram speed of ~1 mm s^{-1}. The extrusion pressure and ram speed were monitored during consolidation. To study the effect of chemically bonded humidity on the powder surface, the cold isostatically pressed powders were subjected to vacuum degassing at 425 °C for 12 h at 3 Pa vacuum prior to extrusion. To study the effect of gas entrapped in the final compacts that was present in the powders during consolidation, vacuum hot unidirectional pressing was performed at 450 °C at 20 Pa vacuum at a pressure of 281 MPa for selected powders prior to extrusion.

Samples were examined using a scanning electron microscope (SEM) FEI Quanta 200 and a transmission electron microscope (TEM) Jeol JEM 200CX. An electron backscatter diffraction (EBSD) was used to measure the crystallographic grain orientations and to determine the mean grain size (d_{EBSD}). The mechanical properties in tension were measured on tensile bars that were machined longitudinally along the extrusion direction; with the gauge of Ø3–30 mm using the ZWICK testing machine at a strain rate of 6×10^{-4} min^{-1}. Tensile tests were performed at room temperature (RT) and at 300 °C. Tensile bars were heated up to 300 °C in 20 min and stabilised for 10 min prior to starting high temperature tensile tests. To study the thermal stability of the compacts, tensile bars of as-extruded compacts were annealed at 300, 450, 500, 550, 600 and 630 °C for 24 h in air prior testing. Dilatometric tests were performed on cylindrical samples with a diameter of 4 mm and a length of 8 mm that were machined longitudinally along the extrusion direction; the tests were carried out in one heating cycle at a heating rate of 1 °C min^{-1} in air using a Linseis L75VS/L81-II machine. The hydrogen content of selected compacts was detected by Horiba EMGA – 830 analyser using graphite crucibles, He atmosphere and the temperature of 2000 °C.

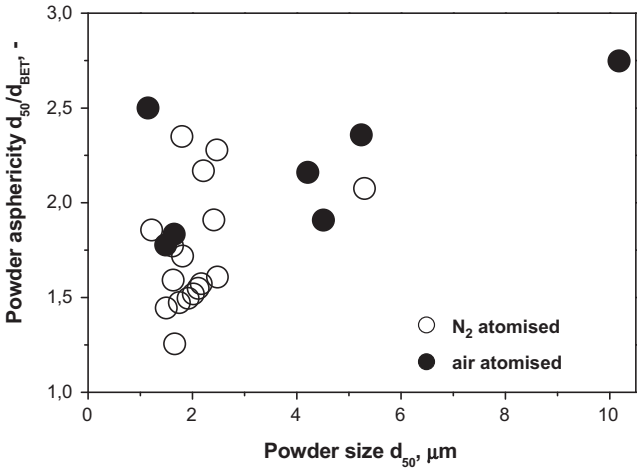

Fig. 1. The asphericity (d_{50}/d_{BET} ratio) of tested powders.

3. Results and discussion

Fig. 1 depicts the surface irregularity of the atomised loose powders using the asphericity (d_{50}/d_{BET} ratio). The atomising atmosphere had no significant influence on the powder asphericity; the

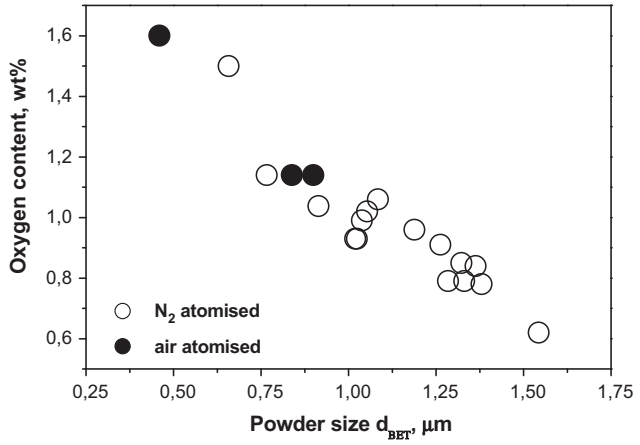

Fig. 2. The oxygen content of the powder as a function of the surface area of the powder (i.e., powder diameter d_{BET}).

Table 1
The properties of as-atomised Al powders.

Powder	Manufacturer	Atomising and collecting atmosphere	d_{50} (μm)	Oxygen (wt%)	BET ($m^2\ g^{-1}$)	d_{BET} (μm)	Al_2O_3 (vol%)
a1	1	Air	1.15	1.6	4.83	0.46	2.3
a2	4	Air	1.49	1.14	2.65	0.84	1.64
a3	4	Air	1.65	1.14	2.47	0.9	1.64
a4	9	Air	4.2	–	1.14	1.95	–
a5	7	Air	4.51	–	0.94	2.36	–
a6	8	Air	5.3	–	1	2.22	–
a7	7	Air	10.18	–	0.6	3.7	–
n1	5	Nitrogen	1.22	1.5	3.38	0.66	2.16
n2	2	Nitrogen	1.5	0.99	2.14	1.04	1.43
n3	11	Nitrogen	1.62	1.04	2.43	0.91	1.49
n4	8	Nitrogen	1.63	0.93	2.17	1.02	1.34
n5	3	Nitrogen	1.66	0.85	1.68	1.32	1.22
n6	5	Nitrogen	1.75	0.96	1.87	1.19	1.38
n7	4	Nitrogen	1.8	1.14	2.9	0.77	1.64
n8	5	Nitrogen	1.81	1.02	2.11	1.05	1.47
n9	6	Nitrogen	1.92	0.79	1.73	1.28	1.14
n10	7	Nitrogen	2.02	0.79	1.67	1.33	1.14
n11	2	Nitrogen	2.1	0.84	1.63	1.36	1.21
n12	5	Nitrogen	2.17	0.78	1.61	1.38	1.12
n13	6	Nitrogen	2.21	0.93	2.18	1.02	1.34
n14	10	Nitrogen	2.37	0.94	–	–	1.35
n15	5	Nitrogen	2.41	0.91	1.76	1.26	1.31
n16	5	Nitrogen	2.47	1.06	2.05	1.08	1.53
n17	5	Nitrogen	2.48	0.62	1.44	1.54	0.89
n18	2	Nitrogen	5.3	0.9	0.87	2.55	1.3

asphericity depended on the powder manufacturer for powders with similar d_{50} values.

An almost linear correlation was observed between the oxygen content of the powder and the measured BET value (or the calculated d_{BET}) regardless of the atomising atmosphere, as shown in Fig. 2. Assuming that all detected oxygen was present in the form of surface Al_2O_3, the thickness of the oxide layer was found not to change markedly. The oxide layer thickness of powders atomised in N_2 was between 1.7 nm and 2.9 nm, as calculated from the oxygen content using d_{BET} and d_{50} values, respectively. For air-atomised powders, the values lied between 1.6 nm and 3 nm. These values were in good agreement with other studies [13–15].

Extrusion of all powder samples yielded sound compacts with densities >99.5% of the theoretical density (THD), which is 2.7 g cm^{-3}. Shear deformation induced during extrusion elongated the Al powder particles and fractured the native oxide layer into separate plate-like dispersoids. Thicknesses of the plate-like dispersoids were given by the thickness of the native oxide layer. Microstructures of the compacts consisted of grains, i.e., powder particles, elongated along the extrusion direction and decorated with nano-metric Al_2O_3 dispersoids introduced in situ. It was previously found that the dispersoids were α-Al_2O_3 [4]. As an example, Fig. 3 shows the transversal and longitudinal cross sections of one compact extruded from a1 powders (d_{50} = 1.15 μm, d_{BET} = 0.46 μm) after deep etching. The Al_2O_3 phase, which had bright contrast, was embedded in the Al matrix, which had dark contrast. As seen in the figure, some small Al particles remained undeformed after extrusion; they kept their initial spherical shape and allowed the Al_2O_3 film to remain continuous. According to previous work, if the powders were extruded at sufficiently low temperatures (i.e., high deformation energy is induced), some Al_2O_3 dispersoids can be found within severely deformed grains [4,12]. However, a relatively high extrusion temperature of 450 °C was used in this study. EBSD maps were obtained for the transversal cross sections of the compacts extruded from four representative Al powders (a1, n11, a4 and a6) and shown in Fig. 4. The mean grain size of the cross sections, or the d_{EBSD} value detected from EBSD maps, is also shown in the figure. The d_{EBSD} values were determined only from large angle grain boundaries. The d_{EBSD} values gradually increased with the increase in the d_{50} value. The number of grains with low angle boundaries increased as the d_{50} value of the powders increased. For the finest a1 powder compacts (d_{50} = 1.15 μm, d_{BET} = 0.46 μm) shown in Fig. 4a, the d_{EBSD} value agreed well with the d_{BET} value. This confirmed that the atomised powder particles were a single grain and maintained as such after extrusion. The single grain structure of this powder was proven previously by TEM (SAED) [4]. It is likely that each grain in the extruded profile was decorated with (broken) oxides that originally covered each powder particle. However, the increasing difference between the d_{BET} value and the d_{EBSD} value in the compacts extruded from larger powder particles (see Fig. 4b–d) indicated the polycrystalline structure of the original powder particle. Some grains in the compacts extruded from larger powder particles were decorated with (broken) oxides that originally covered each powder particle and some grain boundaries free from any surface oxides remained after extrusion. No dominant grain orientation in the transversal cross sections was found, and a statistically random misorientation angle distribution was observed in the grains.

Fig. 5 summarises the tensile strengths (ultimate and yield) and strains of the as-extruded powder compacts at fracture, which were determined at room temperature and at 300 °C as a function of d_{BET}. The atomisation gas had no observable effect on the mechanical properties of the compacts. The strengths of the compacts gradually increased with decreasing d_{BET}, and the strengths increased more noticeably for compacts with d_{BET} values below 1 μm. The tensile strength (UTS), yield stress (YS) and d_{BET} values for the investigated powders correlated well with the relations

$$UTS = a_1 \cdot {d_{BET}}^{-0.27}, \quad (1)$$

$$YS = a_2 \cdot {d_{BET}}^{-0.26}, \quad (2)$$

where the constants a_1 and a_2 at room temperature were calculated as 5.3 and 6, respectively. The constants a_1 and a_2 at 300 °C were calculated as 3.9 and 3.6, respectively. It should be noted that the d_{BET} value for ultrafine powders represented the average size of the starting powder particles more appropriately than the d_{50} value.

Strengthening mechanisms in SAP-like materials were described earlier by Hansen [16]. The strength of the compacts

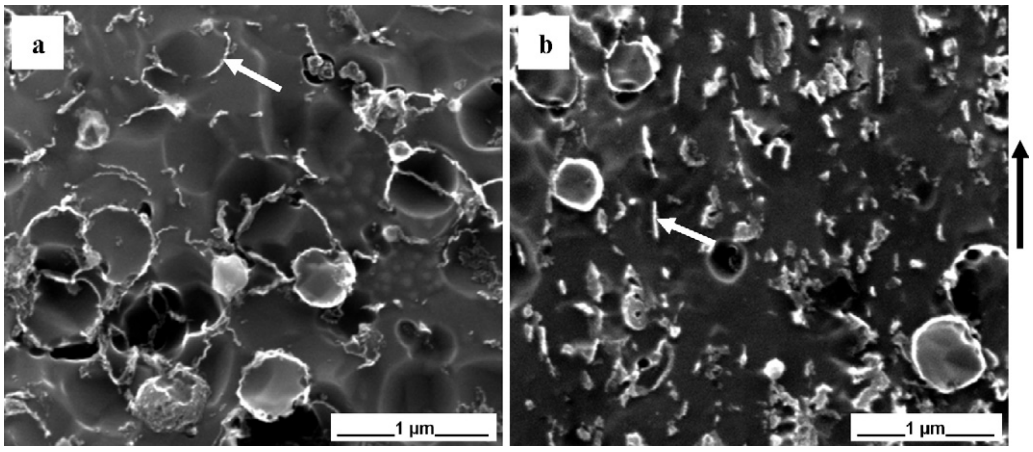

Fig. 3. Secondary electron SEM images of the cross sections of deeply etched compacts in the (a) transversal and (b) longitudinal directions; the compact was extruded from a1 powder (d_{50} = 1.15 μm, d_{BET} = 0.46 μm). White arrows indicate the Al_2O_3 phase. The black arrow indicates the extrusion direction in the longitudinal cross-sectional image.

in this study was a combination of the following strength contributions: dispersion strengthening, large angle grain boundary strengthening, subgrain boundary (low angle grains) strengthening and solid solution strengthening. The effect of solid solution strengthening in technically pure Al alloy powders was negligible relative to the other strengthening mechanisms. Because the dispersoids remained at the grain boundaries after extrusion [4], the typical dispersion strengthening, e.g., by the Orowan mechanism, was negligible in the materials for this study. However, introducing the Al_2O_3 phase enhanced the efficiency of grain boundary strengthening. Similar to the other SAP-like materials, yield strengths (YS) of four chosen powder compacts followed the Hall–Petch relation

$$\mathrm{YS} = \sigma_0 + k \cdot {d_{\mathrm{EBSD}}}^{-0.5}, \quad (3)$$

where σ_0 is the flow stress for an infinite grain size, k is the constant determining the efficiency of grain boundaries as slip barriers and d_{EBSD} is the mean grain size in the transversal direction. Despite the large standard deviation in d_{EBSD} values, a linear correlation in the mean results was obtained with k = 175.4 MPa μm$^{0.5}$ (points 1–4 in Fig. 6). Hansen showed that SAP materials extruded from atomised Al powders featured significantly lower k values of 44–68 MPa μm$^{0.5}$ (lines 6 and 7 in Fig. 6) [16]. This pointed to a higher efficiency of the grain boundaries present in the compacts, which were strengthened with in situ Al_2O_3 dispersoids. The data for the common compact extruded from the coarse Al (99.5%) powder (<400 μm fraction, d_{BET} = 13.07 μm, d_{EBSD} = 6.3 μm) indicated that the efficiency of grain boundaries decreased as k decreased while d_{EBSD} increased (point 5 in Fig. 6).

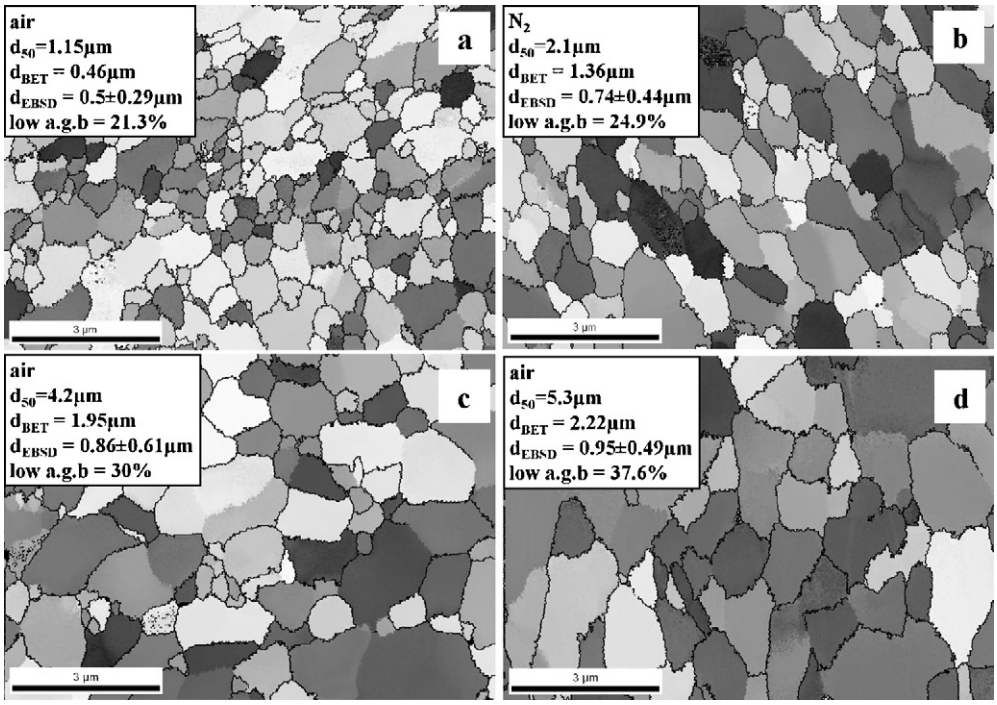

Fig. 4. EBSD maps of transversal cross sections of the compact extruded from four different powders; (a) a1 powder, (b) n11 powder, (c) a4 powder and (d) a6 powder. The atomisation atmosphere, the mean particle diameter (d_{50}), the equivalent particle size calculated from BET (d_{BET}), the transversal grain size obtained from EBSD measurements (d_{EBSD}) and the percentage of low angle grain boundaries (low a.g.b.) for each compact are shown in the insets. Black lines between two adjacent grains represent the large angle grain boundaries.

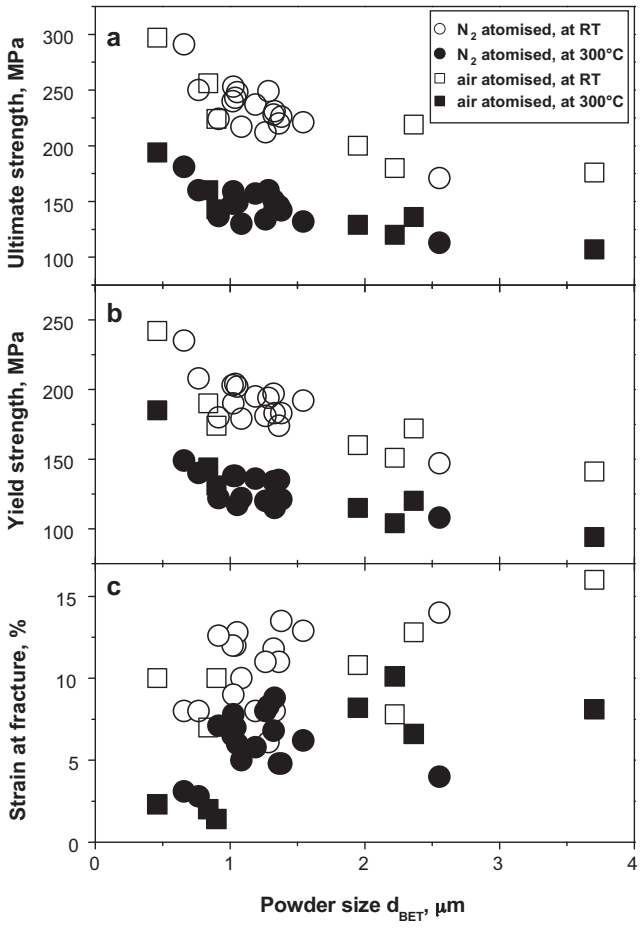

Fig. 5. The effect of the surface area of the powder (i.e., powder diameter d_{BET}) on (a) ultimate tensile strength, (b) yield strength and (c) strain at fracture of extruded compacts (tested at room temperature and at 300 °C).

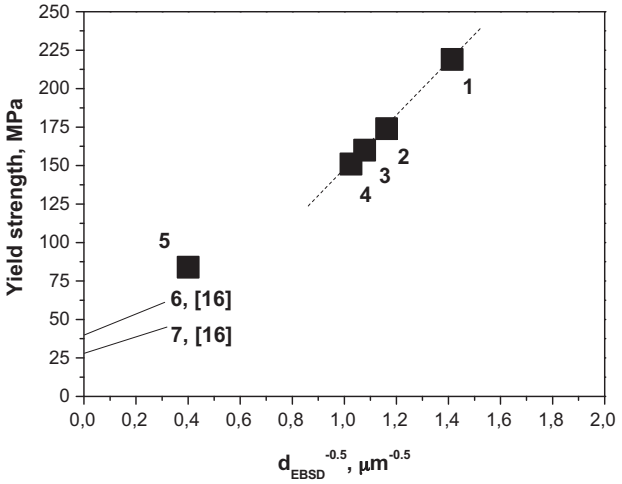

Fig. 6. Room temperature yield strength of four powder compacts (points 1–4) in the as-extruded state as a function of $d_{EBSD}^{-0.5}$ (dotted line). Data for the coarse (<400 μm) size fraction powder compact (point 5) and the extruded compacts studied by Hansen [16] (lines 6 and 7) are included. The extruded compacts are from the following powders: point 1 – a1 powder: d_{50} = 1.15 μm, d_{BET} = 0.46 μm; point 2 – n11 powder: d_{50} = 2.1 μm, d_{BET} = 1.36 μm; point 3 – a4 powder: d_{50} = 4.2 μm, d_{BET} = 1.95 μm; point 4 – a6 powder: d_{50} = 5.3 μm, d_{BET} = 2.22 μm; point 5 – d_{50} = 68 μm, d_{BET} = 13.07 μm; line 6 – SAP material named as Al MD 201, 0.6 wt% Al_2O_3 content; line 7 – SAP material named as Al MD 13, 0.2 wt% Al_2O_3 content.

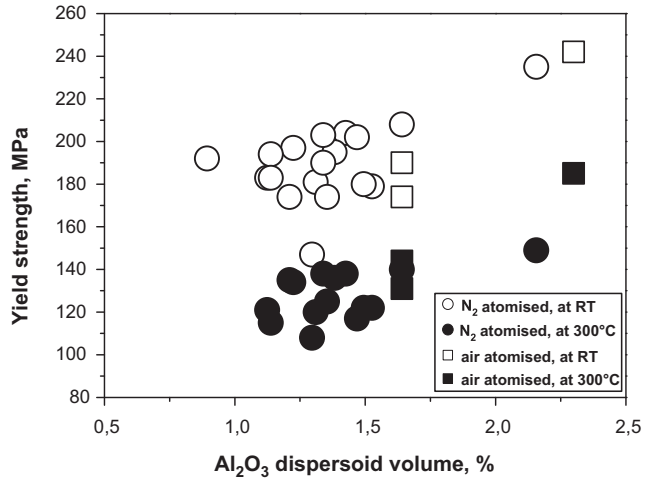

Fig. 7. Yield strength of as-extruded compacts (tested at room temperature and at 300 °C) as a function of Al_2O_3 dispersoid volume.

Fig. 7 depicts the effect of the calculated Al_2O_3 dispersoid amount on the yield strengths of the compacts. Despite the significantly smaller Al_2O_3 volume compared to conventional SAP-like materials, the compacts in this study had a higher yield strength. This was likely due to the presence of nanoscale plate-like Al_2O_3

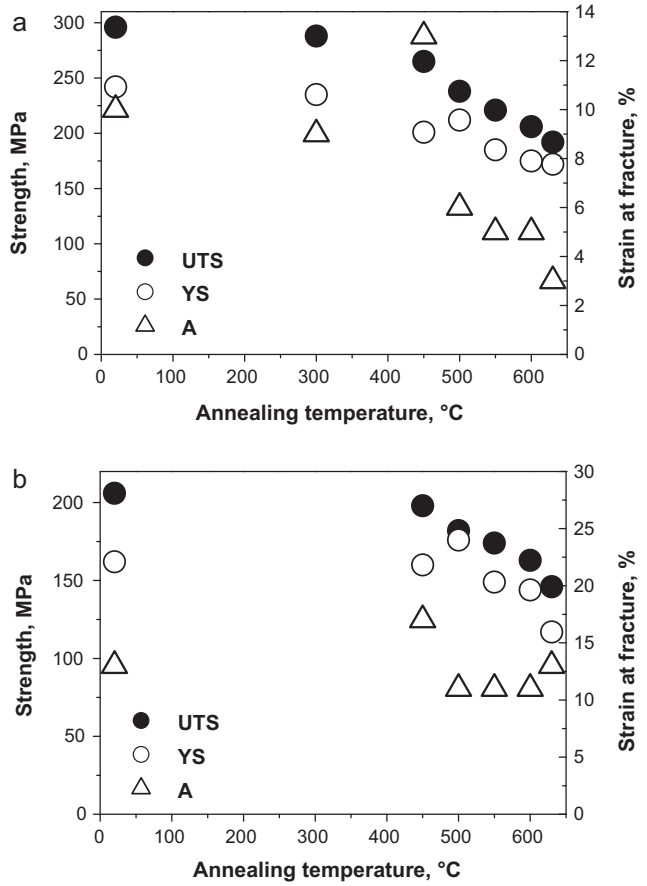

Fig. 8. Mechanical properties of the compacts as a function of annealing temperature; annealing time 24 h (UTS, ultimate tensile strength; YS, yield strength; *A*, strain at fracture). Plot (a) is for compacts from a1 powder (d_{50} = 1.15 μm and d_{BET} = 0.46 μm). Plot (b) is for compacts from n11 powder (d_{50} = 2.1 μm and d_{BET} = 1.36 μm).

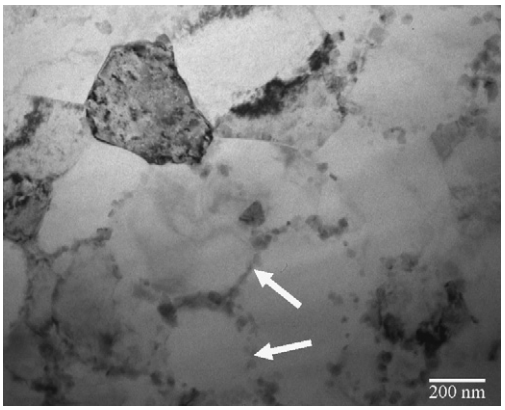

Fig. 9. Bright field TEM image of the transversal cross section of the compact from the a1 powder (d_{50} = 1.15 μm and d_{BET} = 0.46 μm) after annealing for 24 h at 630 °C. White arrows indicate the spherical α-Al_2O_3 dispersoids along the grain boundary of two adjacent grains.

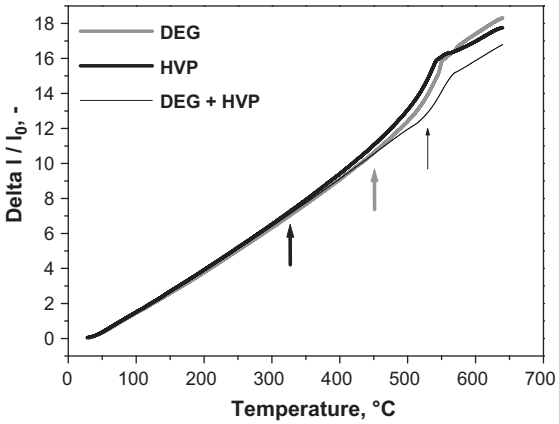

Fig. 10. Dilatometric expansion curves of degassed (DEG), hot vacuum-pressed (HVP) and degassed and hot vacuum-pressed (DEG + HVP) compacts from a1 powder (d_{50} = 1.15 μm and d_{BET} = 0.46 μm). The arrows indicate the onset of expansion due to entrapped gasses.

dispersoids and the ultrafine-grained microstructures in the compacts [16].

As-extruded compacts kept their strength after they were annealed for 24 h at up to ~400–450 °C. Beginning at this temperature, the strength gradually declined as annealing temperatures increased. Fig. 8 shows the thermal stability of two powder compacts (a1 powder: d_{50} = 1.15 μm, d_{BET} = 0.46 μm and n11 powder: d_{50} = 2.1 μm, d_{BET} = 1.36 μm). The strength decreased with increasing annealing temperature as the contribution from individual strengthening mechanisms reduced. In addition, voids formed as a result of entrapped gasses and the escaped humidity. In the first stage of annealing, EBSD measurements confirmed a gradual disappearance of the subgrain structure that led to the initial softening of the compacts. Later, at an annealing temperature of ~500 °C, the shape of the Al_2O_3 dispersoids transformed from a plate-like shape to a spherical shape and remained along the initial grain boundaries [8]. The size of spherical dispersoids was measured to be ~92 nm. The transformation of dispersoids to a spherical shape was accompanied by further strength deterioration. This indicated that the strengthening effect from spherical dispersoids was less efficient compared to that from the plate-like dispersoids, which agreed with our previous findings [8]. Because α-Al_2O_3 is thermodynamically stable at ~500 °C, the mechanism responsible for the morphology change remains uncertain. Similar to the high Al_2O_3 content SAP materials studied by Hansen [16], no obvious signs of massive recrystallisation or grain growth were confirmed by EBSD, even after severe annealing for 24 h at 630 °C. Fig. 9 shows the BF TEM image of the transversal cross section of a1 powder (d_{50} = 1.15 μm, d_{BET} = 0.46 μm) compact annealed at 630 °C for 24 h.

The fracture strain of the compacts dropped as the particle size decreased and the testing temperature increased (Fig. 5). At testing temperatures >500 °C, virtually zero strain was measured at fracture. This phenomenon was consistent with our previous work [8,9,12] and other studies performed on similar SAP-like materials [5]. Reduced fracture resistance at elevated temperatures was speculatively attributed to strain localization and plastic instability between growing microvoids [17]. Because the reduced resistance was explained by dynamic recovery, theories based on the existence of work hardening dislocation cell and source structures in submicron grains were no longer applicable [5]. It should to be pointed out that the reduction in fracture strain at service temperatures >~400 °C in compacts with d_{BET} less than ~1 μm represents a significant drawback in their utilisation.

Table 2
Hydrogen content in the extruded powder compacts.

Powders compacts	d_{BET} (μm)	Condition	Hydrogen (ppm)
a1	0.46	As-extruded	179
a1	0.46	Hot vacuum pressed	131
a1	0.46	Degassed	91
a1	0.46	Degassed + hot vacuum pressed	62
n11	1.36	As-extruded	67
n18	2.55	As-extruded	24

Annealing at <550 °C caused surface blistering of the extruded compacts. In general, fissures and blisters are more prone to appear in compacts of finer powders (despite their small residual porosity) compared to compacts of coarser powders. Table 2 shows that the hydrogen content detected in as-extruded powder compacts (a1, n11 and n18 powders) decreases significantly with increase of d_{BET} value. This could be a reason for the deteriorated fracture strain of the annealed compacts extruded from the finest powders (Fig. 8). Along with subgrain disappearance and dispersoid spheroidisation, the presence of fissures and blisters could be another reason for the deterioration of the fracture strength and strain of compacts annealed at T > 400–450 °C. This finding was consistent with work reported in [16], in which SAP compacts containing more than 10 ppm of gas developed fissures in the microstructure when heated above 400 °C. They found that degassing the finished compacts or loose powders in vacuum at 600 °C or hot pressing of the loose powders in vacuum resolved this problem. We found that degassing the finest CIP a1 powders in vacuum and hot pressing of CIP powders in vacuum led to decrease of compacts hydrogen content from 180 ppm to 90 ppm and 130 ppm, respectively (Table 2). However, degassing or hot pressing the powders in vacuum had no observable effect on the occurrence of blisters or the strength and fracture strain of the powder compacts in this study (both tensile tests were conducted at room temperature and at 300 °C). This observation was supported by dilatometry data of degassed and hot vacuum-pressed compacts of the finest a1 powder, as shown in Fig. 10. A deviation from the linear expansion trend due to the expansion of gasses that were not completely removed during hot vacuum-pressing and degassing is shown. The expansion effect of entrapped gasses in hot vacuum-pressed compacts caused them to expand at ~325 °C. Once the powders were degassed, they expanded at higher temperatures (~470 °C), demonstrating the importance of degassing fine powders. In subsequent cooling and heating cycles, no expansion due to the entrapped gasses was observed. The expansion effect was less pronounced in coarser powders. Insufficient gas removal was likely due to the low degassing (425 °C) temperature and the

short degassing (12 h) time used in this study [18]. However, processing the powders at temperatures greater than ~450 °C under vacuum for a prolonged period of time could trigger the powders to be sintered and cause the mechanical properties to deteriorate [8,19]. Annealing the finished compacts at 600 °C was not feasible because it would enable microstructural changes followed by a decline in strength. Degassing loose powders is extremely dangerous [13,20], especially at an industrial scale. However, vacuum degassing followed by hot vacuum pressing suppressed the occurrence of fissures and blisters significantly in all powder compacts annealed up to 630 °C. Vacuum degassing followed by hot vacuum pressing of a1 powders compacts resulted in further decrease of hydrogen content to 60 ppm (Table 2). Nevertheless, some negative effects of residual gasses were observed above 550 °C in dilatometry tests of the finest a1 powder compacts (Fig. 10). Tensile tests were performed at room temperature, at 300 °C, in as-extruded samples, annealed samples (550, 600 and 630 °C for 24 h), on degassed hot pressed compacts; they proved that the strength and strain at fracture remained unchanged compared with the untreated powder compacts.

4. Conclusions

Twenty-five gas-atomised powders of d_{50} = 1–10 μm were assessed for powder metallurgy purposes. All powders were directly hot extruded into sound compacts. Compacts were composites consisting of an Al matrix reinforced with Al_2O_3 dispersoids formed in situ, which originated from the native oxide film in the powder. It was found that:

- The Al_2O_3 content present on the surface of the as-atomised Al powders had a linear correlation with the surface area of the powders calculated by equivalent BET diameter (d_{BET}).
- The atomising atmosphere had no significant effect on the amount of Al_2O_3 dispersoids introduced and on the mechanical properties of the final compacts.
- The strength of the compacts was closely related to d_{BET}, and the yield tensile strength followed the equation $YS = a_1 \times {d_{BET}}^{-0.26}$ (a_1 = 6 and 3.6 for tests at room temperature and 300 °C, respectively).
- The compacts had relatively high strengths within a broad temperature range. High strengths stemmed from the extraordinary grain boundary strengthening effect in the ultrafine-grained microstructure of the compacts. The efficiency of grain boundary strengthening was significantly enhanced by the presence of nano-metric Al_2O_3 dispersoids introduced in situ. The yield tensile strength followed the relation $YS = -29.3 + 175.4 \times {d_{EBSD}}^{-0.5}$ within the range of particle size tested.
- The extruded compacts showed excellent thermal stability up to ~400 °C. The strength of the compacts deteriorated as the annealing temperature increased due to reduced contribution from the individual strengthening mechanisms.
- The fracture strain of the compacts dropped with decreasing particle size, increasing testing temperature and increasing annealing temperature.
- If high service temperatures are expected of the compacts, the degassed powders should be processed by hot vacuum pressing prior to extrusion to avoid negative effects due to blisters and fissures.

Acknowledgments

The work was supported by funding from MNT-ERA.NET funding. All fine Al powders were supplied by NMD G.m.b.H. The authors thank USTEM (TU Vienna) for the FEG-SEM facility used to characterise the compacts and Dr. J. Dvorak (Institute of Physics of Materials, ASCR) for the help with TEM and EBSD characterisation.

References

[1] R. Irman, Metallurgia 46 (1952) 125–133.
[2] R. Irman, Iron Age (1955) 104.
[3] C.L. Meyers Jr., O.D. Sherby, J. Inst. Met. 90 (1961–1962) 380–382.
[4] M. Balog, F. Simancik, O. Bajana, G. Requena, Mater. Sci. Eng. A 504 (2009) 1–7.
[5] S.S. Kim, M.J. Haynes, R.P. Gangloff, Mater. Sci. Eng. A 203 (1995) 256–271.
[6] W. Xu, X. Wu, T. Honma, S.P. Ringer, K. Xia, Acta Mater. 57 (2009) 4321–4330.
[7] M. Kubota, X. Wu, W. Xu, K. Xia, Mater. Sci. Eng. A 527 (2010) 6533–6536.
[8] M. Balog, C. Poletti, F. Simancik, M. Walcher, W. Rajner, J. Alloys Comp. 509S (2011) S235–S238.
[9] C. Poletti, M. Balog, F. Simancik, H.P. Degischer, Acta Mater. 58 (2010) 3781–3789.
[10] http://www.sapagroup.com/en/Company-sites/Sapa-Profily-as/Our-offer/Research-and-Development/Powder-materials/.
[11] http://www.nmd-gmbh.de/.
[12] M. Balog, J. Nagy, F. Simancik, K. Izdinsky, Int. J. Mater. Prod. Technol. 23 (2005) 1–7.
[13] M.A. Trunov, S.M. Umbrajkar, M. Schoenitz, J.T. Mang, E.L. Dreizin, J. Phys. Chem. B 110 (2006) 13094–13099.
[14] M.A. Trunov, M. Schoenitz, E.L. Dreizin, Propell. Explos. Pyrot. 30 (2005) 36–43.
[15] B. Rufino, F. Boulc'h, M.-V. Coulet, G. Lacroix, R. Denoyel, Acta Mater. 55 (2007) 2815–2827.
[16] N. Hansen, Dispersion-strengthened aluminium products, Risö Report No. 223, 1971, ISBN: 87 550 0059 2.
[17] W.C. Port Jr., R.P. Gangloff, Metall. Trans. A 25 (1994) 365–379.
[18] A. Nylund, Surface Reactions During Atomizing, Handling and Consolidation of Al-Powders, Dissertation Thesis, 1993.
[19] M. Balog, M. Qian, Sintering of fine Al powders, unpublished results.
[20] M. Kearns, Mater. Sci. Eng. A 375–377 (2004) 120–126.